Biodegradable Covalent beta-Cyclodextrin Nanocages for Acidic and Reductive-Responsive Drug Delivery in Enhanced Tumor Therapy

Jingyi Xiao[1], Zan Ge[1], Xiaowei Tan[1], Ziyi Liu[1], Yafang Zhang [1], Shufen Xiao[1], Rongyuan Yi[2], Ye Hu[3], Wenyan Hu[3], Hui Chu[1], and Jian Chen[1]

[1]Hunan University of Science and Technology
[2]Hunan Cancer Hospital
[3]Nanjing Institute for Food and Drug Control

December 05, 2024

Abstract

Traditional beta-cyclodextrin (beta-CD) in biomedical applications faces challenges due to its inherent physical and biochemical limitations. One of the most effective strategies to enhance the properties of beta-CD for drug delivery is the synthesis of supramolecular polycyclodextrins. In this study, we designed a novel beta-CD nanocage-like structure for drug delivery, incorporating imine and disulfide bonds through Schiff base reactions. Aldehyde group-functionalized beta-CD units were used to construct the main backbone of the nanocage, forming dual-dynamic covalent bonds. The chemical structure of the beta-CD nanocage was confirmed using ^{1}H nuclear magnetic resonance (^{1}H NMR) and fourier transform infrared spectroscopy (FTIR). Additionally, atomic force microscopy (AFM) and dynamic light scattering (DLS) revealed that varying amounts of beta-CD crosslinked with cystamine resulted in nanocages approximately 200 nm in size. In vitro drug release experiments demonstrated that doxorubicin (DOX)-loaded beta-CD nanocages exhibited accelerated DOX release in acidic and reductive environments compared to normal physiological conditions, owing to the pH-sensitive imine bond and the glutathione (GSH)-cleavable disulfide bond. The DOX-loaded beta-CD nanocages showed exceptional tumor-killing effects, particularly in acid/reduction-enhanced tumor cells. Both cellular fluorescence imaging and flow cytometry confirmed the potential of the beta-CD nanocages for acid/reduction-specific drug release. Consequently, this precision medicine model using imine/disulfide-linked beta-CD nanocage structures as acidity/reduction-sensitive drug carriers promises to improve oncotherapy through more targeted drug delivery and release, supporting individualized treatment approaches.

1. Introduction

Beta-CD is a unique amphiphilic cyclic macromolecule characterized by the presence of multiple hydroxyl groups, making it broadly applicable across various scientific fields, particularly in biomedicine, chemistry, food science, and environmental science1[]. Beta-CD has a distinct bucket-shaped cavity with an inner diameter and depth of approximately 0.8 nm each. This macrocyclic feature provides a versatile foundation for the construction of beta-CD/drug inclusion complexes, which are primarily driven by van der Waals forces, hydrogen bonding, and hydrophobic interactions2[]. The capacity to encapsulate potential pharmaceutical molecules enhances their bioavailability, masks odors, improves water solubility, and reduces drug toxicity. Consequently, beta-CD can mitigate undesirable properties of pharmaceutical compounds due to these characteristics. As a result, this field is rapidly advancing in drug delivery and bioavailability by leveraging beta-CD's host–guest interactions and selective modifications3[].

In recent years, with the rise of intelligent drug delivery systems and advancements in biomedical materials, the design and assembly of drug carriers have become increasingly complex, hindering clinical translation4[].

Dual and multi-stimuli-responsive beta-CD nanoparticles, developed through various chemical modifications, are continuously emerging. Despite significant progress, many intelligent beta-CD drug delivery techniques remain at the conceptual and laboratory stages, impeding practical applications. As beta-CD supramolecular structures become more intricate, the number of uncontrollable factors increases significantly. Furthermore, challenges in beta-CD-based drug delivery systems are mainly due to a lack of understanding of in vivo catabolism and behavior. However, researchers are actively addressing these issues to develop clinical and translational solutions for effectively treating various tumors. Simple and effective drug delivery systems are gaining attention for their optimal therapeutic effectiveness, achieved through rational and biomimetic design5[]. For controlled release drug carriers, the regulation of drug release behavior, including timing and dosage, should respond to external stimuli. Overall, drug carriers can modulate drug release based on stimulus intensity, which includes endogenous stimuli (e.g., pH, redox, and enzymes)6-10[] and exogenous stimuli (e.g., temperature, light, and ultrasound)11[].

The design of topologically intriguing beta-CD macromolecular architectures plays a critical role in enhancing drug release behavior, simplifying complex systems, and improving drug load capacity, colloidal stability, and hydrophilic and hydrophobic properties, primarily due to the versatility of beta-CD. Notably, the hydrophilic and hydrophobic properties are improved by several magnitudes. Classes of beta-CD topologies, including cage-like, chain-like, bridged structures, polyrotaxanes, and star/multi-arm polymer nanostructures, are unique not only from a topological geometry perspective but also in their relevance to programmed drug delivery12[]. These structures are promising candidates for forming inclusion complexes with guest molecules, enabling effective drug encapsulation. Various medicinal molecules, such as antitumor drugs, anti-diabetic drugs, anti-inflammatory agents, and antihypertensive drugs, have been encapsulated in beta-CD-based topology systems for long-term release13-17[]. Recent studies have shown that functionalizing beta-CD can significantly improve application outcomes. For example, Zhang et al. developed an acid-sensitive poly(beta-CD)-based multifunctional supramolecular gene vector, consisting of poly(beta-CD) as the backbone and acetal bond-linked PGEA as the arms through atom transfer radical polymerization (ATRP) and ring-opening reactions18[]. Chen et al. proposed a multicharge beta-CD supramolecular assembly based on an amphiphilic beta-CD bearing seven hexylimidazolium units, which demonstrated specific cancer cell targeting and controlled drug release abilities19[]. Colesnic et al. designed difunctionalized beta-CD to create a porous organic hierarchical supramolecular assembly through regioselective functionalization, resulting in a porous organic architecture20[]. The performance of beta-CD macromolecules is enhanced by strong intramolecular interactions within beta-CD fragments. Consequently, there is an urgent need for simple and efficient methods to develop beta-CD macromolecular architectures that extend the physicochemical performance and drug loading behavior of beta-CD2122[,]. In particular, long-range interactions between beta-CD fragments are utilized to build cage-like, chain-like, and bridged structures.

Due to its large-ring structure and multiple hydroxyl groups, beta-CD is an excellent material for potential polymer crosslinking network structures. Consequently, we designed a nanocage-like drug carrier using beta-CD as the molecular building blocks and imine/disulfide bridges as switchable units in a straightforward manner. The network structure facilitates the distribution of hydrophobic pharmaceutical molecules within the nanocage-like space through host-guest and hydrophobic interactions, enhancing drug loading and delivery. Additionally, the proposed beta-CD nanocage exhibited a nano-sized structure with triggered doxorubicin (DOX) release in response to acidic and reductive environments. Overall, the assembly of the beta-CD supramolecular structure becomes significantly simpler, and uncontrollable factors are greatly reduced23[]. This drug delivery system adheres to the fundamental principle of treating the correct patient, at the right time, with the precise drug dose, potentially improving treatment outcomes for various diseases.

Hosted file

`image1.wmf` available at https://authorea.com/users/867469/articles/1247771-biodegradable-covalent-beta-cyclodextrin-nanocages-for-acidic-and-reductive-responsive-drug-delivery-in-enhanced-tumor-therapy

Figure 1 Schematic illustration of the assembly process and acidity/reduction-sensitive drug delivery me-

chanism of biodegradable covalent beta-CD nanocages for tumor therapy.

2. Experimental

2.1. Materials and Methods

Beta-CD, dimethyl sulfoxide (DMSO), and 2-iodoxybenzoic acid (IBX) were purchased from ENERGY-CHEMICAL (Shanghai, China). Copper (II) hydroxide (Cu(OH)2), cystamine, sodium acetate, methanol (MeOH), and doxorubicin (DOX) were obtained from Aladdin Corporation (Shanghai, China).^{1}H NMR analyses were carried out using a Bruker ADVANCE 400 MHz Spectrometer (Germany). FTIR measurements were conducted in transmission mode at room temperature, covering the range of 400 to 4000 cm-^{1}. AFM was performed in tapping mode using a Bruker Dimension ICON, with a scan rate of 1 Hz and a scan size of 1 μm × 1 μm. Size distribution was analyzed using a ZEN 3600 dynamic light scattering (DLS) instrument from Malvern.

2.2 Synthesis of aldehyde group functionalized beta-CD

Beta-CD (11.35 g, 10 mmol) was dissolved in 20 ml of DMSO and stirred until the solution became clear. The oxidizing agent, IBX, was gradually added to the solution at a reaction temperature of 40 °C. Fresh Cu(OH)2 was used to detect the presence of aldehyde groups. The reaction progress was monitored by thin-layer chromatography (DCM: MeOH = 20:1). After 48 hours, the reaction mixture changed from a colorless, transparent liquid to a white, turbid liquid, indicating completion. The resulting solution was poured into water and vacuum filtered to remove excess IBX and water-insoluble solids. The filtrate was then transferred to a dialysis bag (MWCO 500) and dialyzed in water for three days. Finally, the product was freeze-dried to yield a white solid (6.62 g, 58%) for further use.

2.3 Synthesis of beta-CD nanocage

Cystamine dihydrochloride (0.450 g, 2 mmol) and sodium acetate (0.164 g, 2 mmol) were dissolved in a MeOH (4 ml)/H2O (1 ml) solution. The mixture was stirred at 40 °C for 20 minutes until it became clear and transparent. Next, aldehyde group-functionalized beta-CD (3.459 g, 3 mmol) and MeOH (10 ml) were added to the solution, which was then stirred for 18 hours. The reaction progress was monitored by thin-layer chromatography (TLC). The resulting solution was subjected to vacuum filtration and concentrated, yielding a brown oil. This oil was allowed to stand for three days, resulting in the precipitation of yellow acicular crystals (1.56 g, 40%).

2.4 Preparation of DOX-loaded beta-CD nanocage

Beta-CD nanocages (100 mg) were dissolved in 5 ml of PBS solution (pH 7.4). DOX (100 mg) was dissolved in 1 ml of DMSO and added to the beta-CD nanocage solution using a microsyringe. The solution was stirred in the dark for 12 hours. Subsequently, the solution was transferred to an Amicon centrifuge tube (MWCO 3000, Merck Millipore, USA) for concentration and washed three times with PBS to remove unloaded DOX. The final residue was freeze-dried.

2.5 Drug assay and release of DOX-loaded beta-CD nanocage

A series of standard DOX stock solutions were prepared, and a standard curve was obtained by measuring the absorbance using a plate reader with a 485 nm excitation filter and a 538 nm emission filter (Thermo Scientific Fluoroskan Ascent FL). Based on the standard curve equation y = 0.04464*x + 0.02131, the drug loading capacity of the beta-CD nanocages was determined to be 37.5% using the formula: the beta-CD nancage drug loading capacity=the loaded DOX content/(the loaded DOX content+beta-CD nanocage content)*100%.

pH 4.5 PBS solution was used to mimic the acidic tumor microenvironment, while a 5 mM GSH solution simulated the reductive tumor microenvironment. pH 7.4 PBS solution was used to represent the normal physiological environment. DOX-loaded beta-CD nanocages (20 mg) were dissolved in each of these three types of solutions (1 ml) and poured into separate Amicon centrifuge tubes. These tubes were then immersed

in larger tubes containing the respective release medium (5 ml) and placed in an incubator shaker at 100 rpm at 37 °C. Aliquots were taken from the release medium at predetermined time intervals, and an equal volume of fresh buffer was added each time. The samples were measured using a plate reader with a 96-well plate.

2.6 Biocompatibility of beta-CD nanocage and cell killing effect of DOX-loaded beta-CD nanocage

SKOV-3 cells were cultured in RPMI 1640 medium (Gibco) supplemented with 10% fetal bovine serum (Gibco), 100 μg/ml penicillin (Sigma-Aldrich), and 100 μg/ml streptomycin (Sigma-Aldrich) at 37 °C with 5% CO_2. The cells were seeded in a 96-well plate at a density of 10,000 cells/well in 100 μl of culture medium. After 12 hours, the culture medium was replaced with 100 μl of fresh culture medium containing different concentrations of beta-CD nanocages for 12 hours. Cell viability was assessed using a CCK-8 assay (Solarbio).

For the cell killing rate test, SKOV-3 cells in a 96-well plate were pretreated with pH 4.5 PBS (100 μl), 5 mM GSH (100 μl), and pH 7.4 PBS (100 μl) for 2 hours. Subsequently, 100 μl of fresh culture medium containing different concentrations of DOX-loaded beta-CD nanocages was added and incubated for 12 hours. Cell viability was evaluated using a CCK-8 assay.

2.7 Fluorescence imaging of coumarin 6-loaded beta-CD nanocage

The preparation of coumarin 6-loaded beta-CD nanocages followed a similar procedure to that of DOX-loaded beta-CD nanocages. SKOV-3 cells were seeded in 6-well plates at a density of 1×10^6cells/well in 2 ml of culture medium. After 12 hours of culture, the cells were pretreated with pH 4.5 PBS (1 ml), 5 mM GSH (1 ml), and pH 7.4 PBS (1 ml) for 2 hours. Subsequently, 1 ml of fresh culture medium containing coumarin 6-loaded beta-CD nanocages with an equivalent coumarin 6 concentration of 112.5 ng/mL was added, and the cells were incubated for 3 and 6 hours, respectively. Finally, the cells were washed thrice with PBS, and fluorescence images were captured using an Olympus IX 73 microscope.

2.8 Flow cytometry analysis of coumarin 6-loaded beta-CD nanocage

SKOV-3 cells were seeded in 6-well plates at a density of 1×10^6 cells/well in 2 ml of culture medium. After 12 hours of culture, the cells were pretreated with pH 4.5 PBS (1 ml), 5 mM GSH (1 ml), and pH 7.4 PBS (1 ml) for 2 hours. Subsequently, 1 ml of fresh culture medium containing coumarin 6-loaded beta-CD nanocages with an equivalent coumarin 6 concentration of 112.5 ng/mL was added, and the cells were incubated for 3 and 6 hours, respectively. Finally, the cells were collected by trypsin digestion and analyzed using a flow cytometer (COULTER EPICS XL, Beckman, USA). The data were analyzed using FlowJo software.

3. Results and discussion

3.1 Physical and chemical properties of beta-CD nanocage

An acidity/reduction-sensitive beta-CD nanocage was assembled using cystamine dihydrochloride via a Schiff base reaction. The unique structural unit of the nanocage was the aldehyde group-functionalized beta-CD. To obtain this unit, a mild and efficient oxidation of the OH-6 of beta-CD was carried out at room temperature using IBX, resulting in excellent yields. Figure 2 shows the ^{1}H NMR spectroscopy analysis of the pre- and post-oxidation of beta-CD. The chemical shifts of protons in the glucose units of the primitive beta-CD were observed, such as 5.75 (OH-2), 5.69 (OH-3), 4.83 (H-1), 4.47 (OH-6), 3.63 (H-6a,b), 3.57 (H-3), 3.55 (H-5), 3.34 (H-4), and 3.30 (H-2). After oxidation, new peaks appeared at 9.5 ppm, and the OH-6 peaks weakened at 4.47 ppm, which were attributed to the aldehyde proton peaks24[]. Comparison of the results indicated the successful preparation of aldehyde group-functionalized beta-CD using IBX oxidation. Subsequently, we used cystamine to crosslink the aldehyde group-functionalized beta-CD via an aldehyde-amine reaction. As shown in Figure 2 (c), the aldehyde proton peaks at 9.5 ppm disappeared, indicating the nearly completed reaction between the aldehyde of beta-CD and the amino group of cystamine. The^{1}H NMR spectrum of cystamine is shown in Figure S1. Due to the stacking of multiple glucose units, the proton peaks overlapped

rather than appearing as distinguishable peaks in beta-CD. After being loaded with doxorubicin (DOX), the benzene ring peak of DOX (7-8 ppm) could be partially observed, but the majority of DOX proton peaks were shielded by the beta-CD nanocage. Meanwhile, the ^{1}H NMR spectrum of DOX is shown in Figure S1.

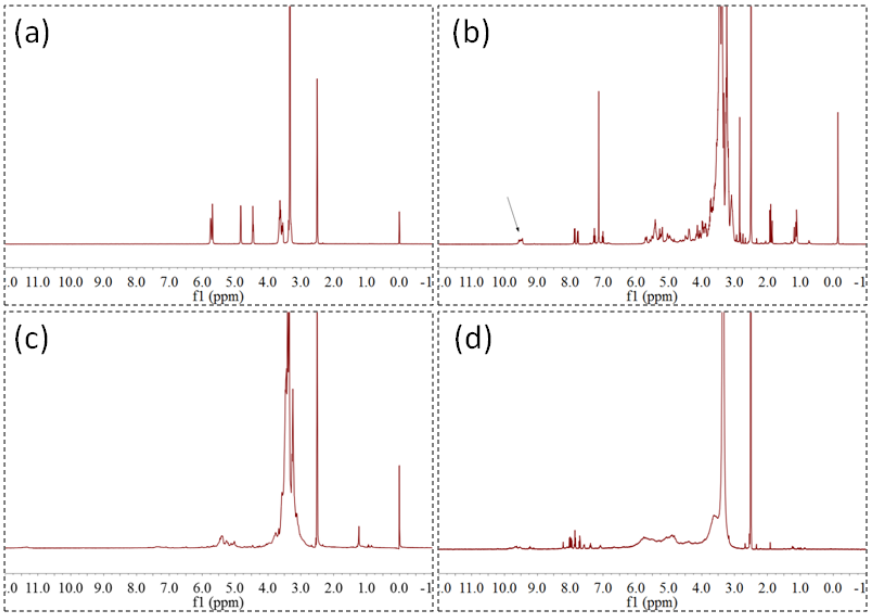

Figure 2 ^{1}H NMR data of beta-CD (a), aldehyde group functionalized beta-CD (b), crosslinked beta-CD nanocage (c) and crosslinked beta-CD nanocage loaded with DOX (d).

The assembly process of the beta-CD nanocage was further examined using FTIR. For beta-CD, the broad peaks at 3300 cm^{-1} and 1420 cm^{-1} are assigned to the OH stretching and bending vibrations, respectively. The absorption peak at 2920 cm^{-1} corresponds to CH stretching vibrations, while the prominent peak at 1020 cm^{-1} is attributed to the CO stretching vibration of the glucose unit25[]. Upon oxidation of beta-CD, a clear characteristic peak at 1740 cm^{-1} emerged, corresponding to the C=O stretching vibration of the CHO group2426[,]. Another prominent peak at 2730 cm^{-1} is associated with the CH stretching vibrations of the CHO group. Other characteristic peaks remained relatively unchanged compared to pure beta-CD. After crosslinking with cystamine, the characteristic peak of the CHO group weakened, indicating the reaction between the aldehyde group-functionalized beta-CD and cystamine. Additionally, two new absorption peaks appeared at 1650 cm^{-1} and 570 cm^{-1}, respectively assigned to the C=N stretching vibration and the SS bond, indicating the successful introduction of the acid-sensitive imine and reduction-sensitive disulfide bonds. Following the loading of DOX into the beta-CD nanocage, the DOX signal was observed, including the absorption peak at 3000 cm^{-1}assigned to the CH stretching vibrations of the DOX benzene ring, the absorption peak at 3300-3500 cm^{-1} assigned to the OH and NH stretching vibrations of DOX, the absorption peak at 1750 cm^{-1} assigned to the C=O stretching vibration, and the absorption peaks at 1650 cm^{-1} and 1500 cm^{-1} assigned to the C=C stretching vibration of the benzene skeleton. The FTIR spectrum of pure DOX is also provided in Figure S2. Some characteristic peaks overlapped between DOX and the beta-CD nanocage, but the loaded DOX signals were distinguishable27[]. Through the combination of FTIR and ^{1}H NMR analysis, we were able to identify the components of the beta-CD nanocage and its derivatives.

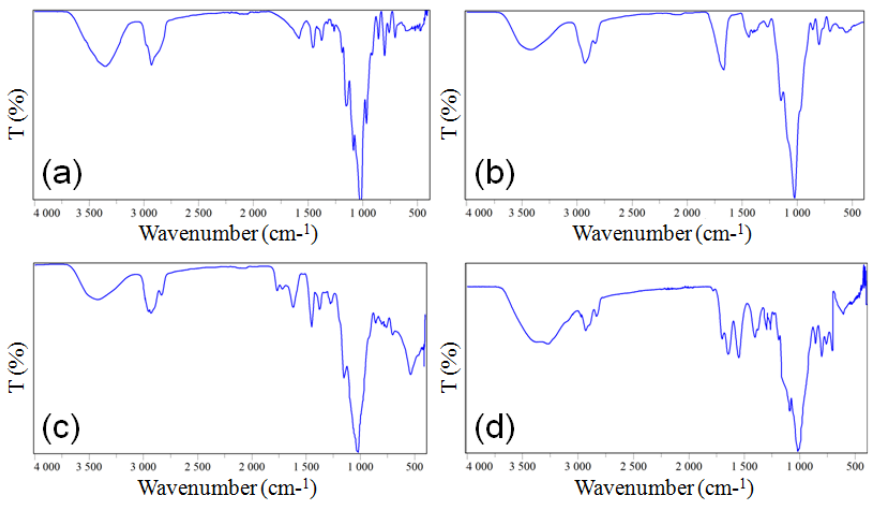

Figure 3 FTIR analysis of beta-CD (a), aldehyde group functionalized beta-CD (b), crosslinked beta-CD nanocage (c) and crosslinked beta-CD nanocage loaded with DOX (d).

The size of the beta-CD nanocage plays a crucial role in determining the endocytosis pathways for internalizing these nanoparticles into tumor cells. Therefore, the size and evolution process of the beta-CD nanocage were investigated using AFM. First, the size of pristine beta-CD was examined. As shown in Figure 4, the size of individual beta-CD molecules appeared small, with a diameter of approximately 10 nm. However, the larger size observed in the AFM image might be attributed to agglomeration of the molecules. Following the oxidation process, the size of beta-CD showed slight variation, but the agglomeration phenomenon persisted. After crosslinking with cystamine, the resulting nanocage-like structure of beta-CD exhibited a larger size compared to the individual beta-CD, with sizes ranging between 100 nm and 200 nm. It is noted that there was an oversizing of the beta-CD nanocage due to the induced agglomeration between beta-CD molecules. More importantly, after drug loading, DOX-loaded beta-CD exhibited an appropriate size (100-200 nm) for endocytosis. The size of DOX-loaded beta-CD was similar to that of unloaded beta-CD nanocage. This suggests that the physical size of the prepared nanocage could essentially meet the requirements for endocytosis2829[,].

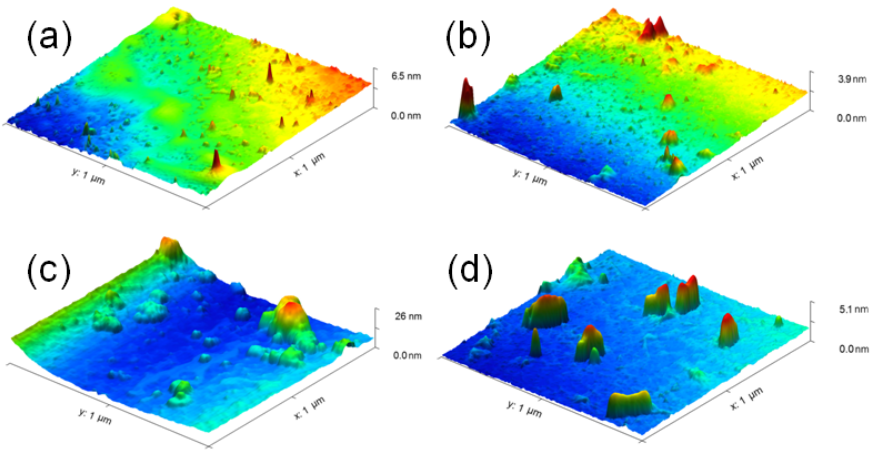

Figure 4 AFM image of beta-CD (a), aldehyde group functionalized beta-CD (b), crosslinked beta-CD

nanocage (c) and crosslinked beta-CD nanocage loaded with DOX (d).

The hydrated state of beta-CD reflects its true state in the physiological environment and its subsequent effects on endocytosis pathways. Therefore, DLS was used to evaluate the hydrated size of the beta-CD nanocage. Simultaneously, the change in hydrated size could also reflect the self-assembly process. As shown in Figure 5, the hydrated size of individual beta-CD and aldehyde group-functionalized beta-CD was approximately 20 nm, and the size distribution was relatively stable. Upon assembly with cystamine, the size gradually increased to over 100 nm for the beta-CD nanocage. The size distribution of the beta-CD nanocage exhibited a wider range compared to free beta-CD. One reason for this outcome might be the crosslinking of beta-CD, resulting in a larger spatial structure. Additionally, the crosslinking process may not guarantee the same quantity of beta-CD units every time, leading to imbalanced crosslinked units. After loading with DOX, the beta-CD nanocage still exhibited an appropriate hydrated size of around 200 nm, indicating that the structure of beta-CD remained stable even when loaded with a hydrophobic drug. The size distribution of the DOX-loaded beta-CD nanocage was similar to that of the unloaded beta-CD nanocage. These DLS results suggest that the trends in hydrated size change of beta-CD in different states were similar to the trends in dehydrated size change provided by AFM.

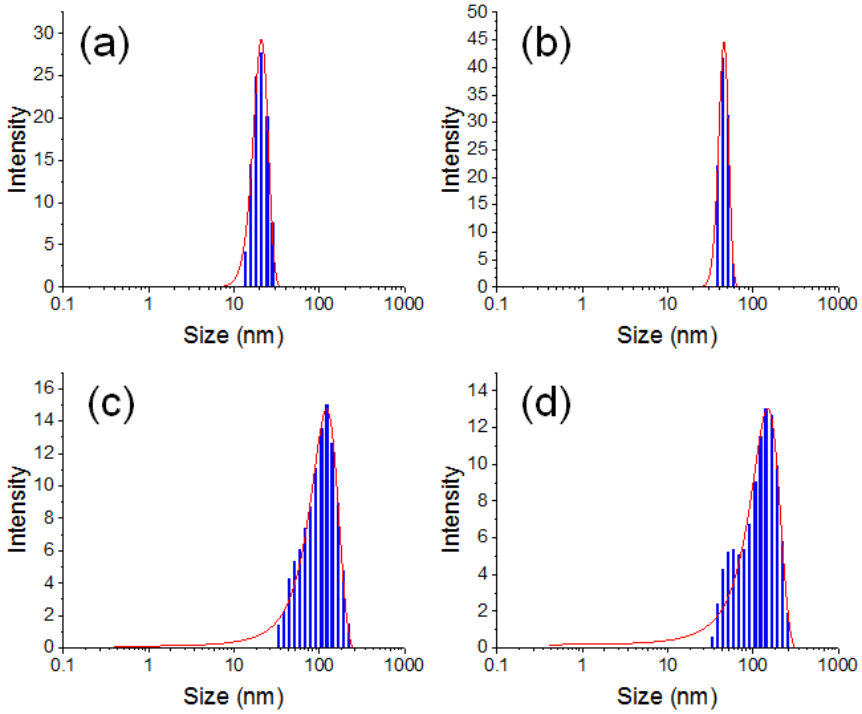

Figure 5 The hydrodynamic diameters of beta-CD (a), aldehyde group functionalized beta-CD (b), crosslinked beta-CD nanocage (c) and crosslinked beta-CD nanocage loaded with DOX (d).

3.2 Self-regulate drug release of beta-CD nanocage in mimic tumor microenvironment

In this beta-CD nanocage, cystamine was used as a crosslinker in a simple manner to assemble this nanostructure, benefiting from its disulfide bond and amino groups at the two ends. This property makes it convenient to react with the aldehyde group-functionalized beta-CD. The new covalent framework with imine and disulfide bonds has been established, but its acidity/reduction-sensitive performance remained unclear. Therefore, understanding the acidity/reduction-responsive release of drugs is crucial for determining their impact on enhancing anti-tumor efficiency. To investigate the acidity/reduction-responsive drug release, pH 4.5 PBS solution and 5 mM GSH solution were used to mimic the acidic and highly reductive

tumor microenvironments, respectively. In the acidic-mimic environment, the beta-CD nanocage exhibited a rapid drug release rate (over 60% drug release in conjugation of imine contributed to bond fission in an acidic environment. This led to the disassembly of the beta-CD nanocage and the release of DOX from the enclosed nanocage. In the GSH-mimic environment, the DOX release rate from the beta-CD nanocage increased (over 60% drug release in ˜25 h) but was weaker compared to the acidic-mimic environment, suggesting that the controllable breakage of disulfide bonds was mediated by GSH. More importantly, the beta-CD nanocage exhibited weak release even after 50 h in a normal physiological environment. This contrasted markedly with its controllable drug release under acidic/GSH stimuli. Additionally, the hydrodynamic diameters of the DOX-loaded beta-CD nanocage treated with acidic and reductive agents, as well as neutral solutions, were measured (Figure S3). The change in hydrodynamic diameters was more pronounced when the DOX-loaded beta-CD nanocage was treated with acidic and reductive agents, indicating easier disintegration of the beta-CD nanocage structure in acidic and reductive environments. Therefore, the stimuli-responsive properties of the beta-CD nanocage were ultimately attributed to the covalent imine and disulfide bonds.

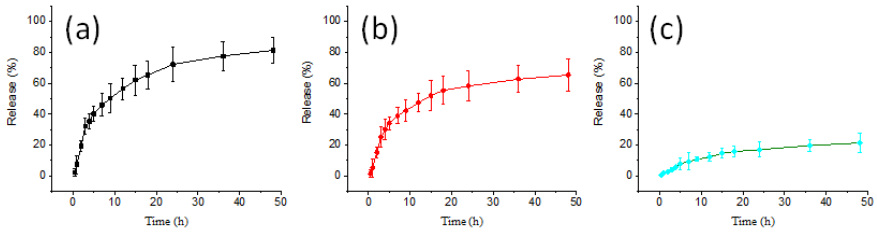

Figure 6 The release curves of DOX-loaded beta-CD nanocage in acidic environment (pH 4.5 PBS) (a), reduction environment (5 mM GSH) (b) and normal physiological environment (pH 7.4 PBS) (c).

3.3 The cytocompatibility of drug-free beta-CD nanocage and cell-killing effect of DOX-loaded beta-CD nanocage

After confirming the structure, characterizing the size, and testing the drug release performance, the cytocompatibility of drug-free beta-CD nanocage and the cell-killing effect of DOX-loaded beta-CD nanocage were further evaluated in vitro using a CCK-8 method. As shown in Figure 7, drug-free samples demonstrated good biocompatibility with over 80% cell viability at a concentration of 800 ng/ml. This result suggests that the composition of the beta-CD nanocage is almost non-toxic. Efficient delivery of DOX to tumor cells and killing tumor cells are crucial for using this proposed beta-CD nanocage. Therefore, SKOV 3 cells were incubated in acidic, GSH, and normal environments to verify the cell-killing effect of DOX-loaded beta-CD nanocage. In the acidic culture environment, DOX-loaded beta-CD nanocage exhibited an outstanding cell-killing effect with an IC50 of 600 ng/ml DOX-loaded beta-CD nanocage, equivalent to a DOX concentration of 225 ng/mL. In the GSH culture environment, DOX-loaded beta-CD nanocage also showed a superior cell-killing effect (IC50 of 700 ng/ml DOX-loaded beta-CD nanocage) but lower than in the acidic culture environment. In the normal culture environment, DOX-loaded beta-CD nanocage demonstrated a lower cell-killing effect. The proposed beta-CD nanocage with acid/reduction-responsive properties stands out from the normal physiological environment. When free DOX was directly treated with Skov 3 cells, the cell-killing rate was the highest, as shown in Figure 7(f), with the tumor cells exhibiting the lowest cell viability. These cell killing tests suggest that the beta-CD nanocage can self-regulate drug release, especially in the tumor microenvironment, effectively avoiding nonspecific release. Additionally, the beta-CD nanocage improved the drug release behavior in the tumor microenvironment to minimize toxicity to normal cells and maximize the anti-tumor effect.

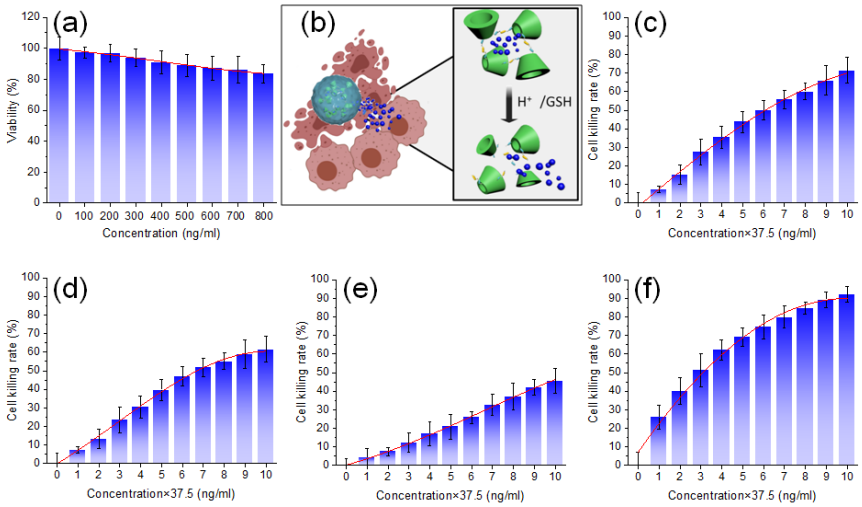

Figure 7 In vitro biocompatibility of beta-CD nanocage (a). Schematic illustration of drug release of beta-CD nanocage in the acidic and reductive microenvironment of tumor cell (b). In vitro antitumor effect of DOX-loaded beta-CD nanocage in acidic environment (c), reduction environment (d) and normal physiological environment (e) as well as the in vitro antitumor effect of free DOX (f).

3.4 Intracellular fluorescence imaging analysis of coumarin 6-loaded beta-CD nanocage

To determine whether the beta-CD nanocage could enhance DOX release in acidic or GSH-specific cellular microenvironments, intracellular fluorescence imaging was conducted to evaluate the two distinct responsive properties of the beta-CD nanocage. Tumor cell environments were induced to intensify acid and GSH expression. Specifically, in acid-treated tumor cells, green fluorescence was evident at 3 h and continued to increase at 6 h, indicating that H^+triggered the breakage of imine bonds, causing the nanocage to gradually disintegrate and release coumarin 6. When tumor cells were treated with GSH, the green fluorescence signal was also evident and increased over time, indicating that disulfide bonds also underwent breakage in the enhanced reducing environment, allowing coumarin 6 to escape from the beta-CD nanocage. In untreated tumor cells, the fluorescence was lower compared to acid- or GSH-treated tumor cells, and the contrast between treated and untreated groups was noticeable. These results demonstrated that beta-CD is highly sensitive to acidic and GSH environments. Therefore, the enhanced intracellular drug release and uptake could be improved using this proposed beta-CD nanocage.

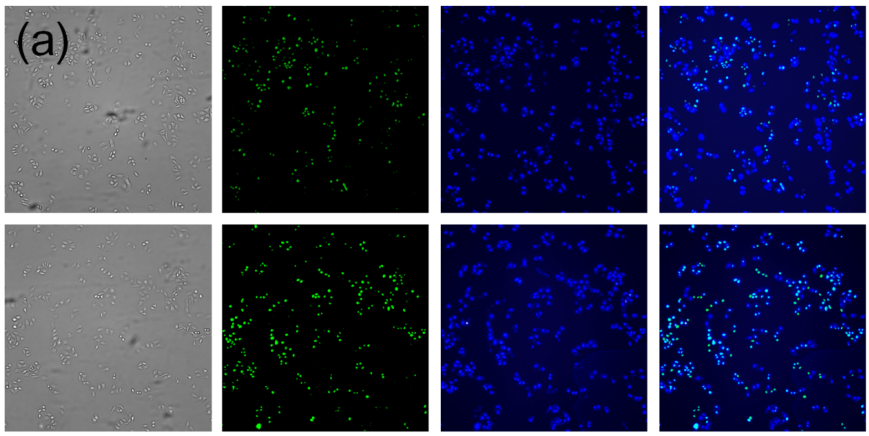

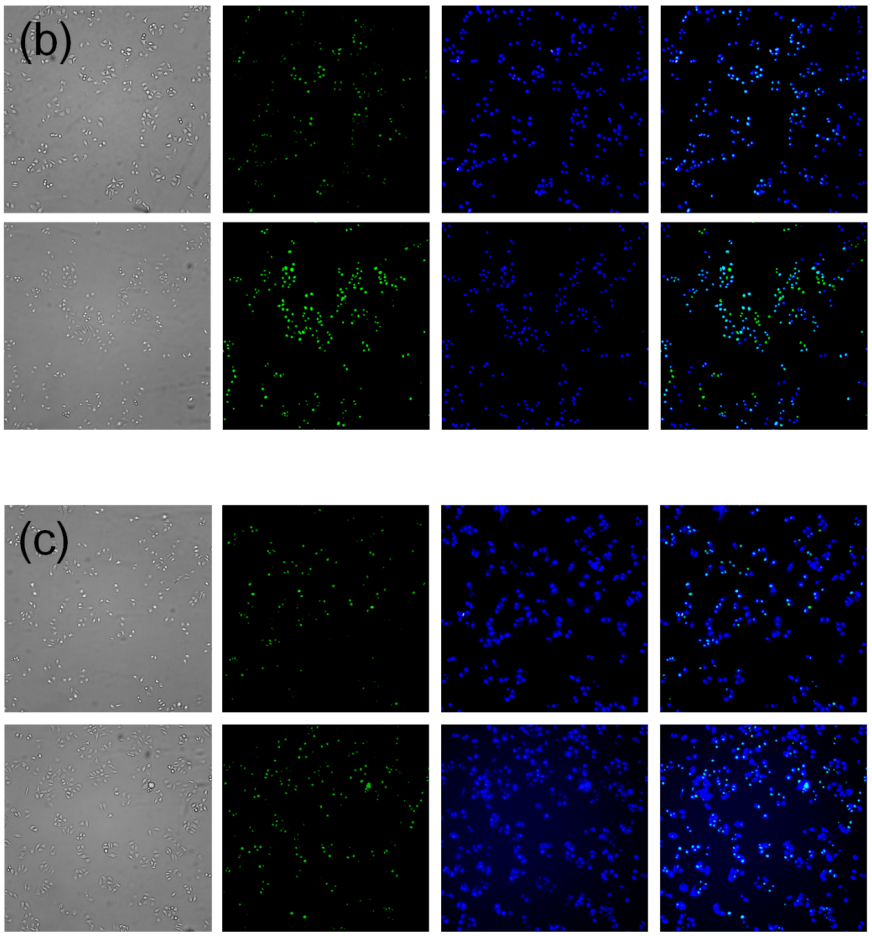

Figure 8 The fluorescence imaging analysis for treating SKOV3 cells with coumarin 6-loaded beta-CD nanocage in acidic environment for 3 h and 6 h (a), reduction environment for 3 h and 6 h (b) and normal physiological environment for 3 h and 6 h (c) respectively.

3.5 Flow cytometry analysis of coumarin 6-loaded beta-CD nanocage

The beta-CD nanocage, containing dual-dynamic covalent bonds based on imine and disulfide, played a critical role in controlling drug release. Maintaining the superior performance of beta-CD with specific release properties remains a driving force for further exploration. Therefore, further evidence from flow cytometry analysis was employed. Similar to cell fluorescence imaging, tumor cells were treated with upregulated acidity, upregulated GSH, or left untreated before flow cytometry analysis. As shown in Figure 9, the relative fluorescence intensity increased from untreated tumor cells to GSH-treated tumor cells and further to acid-treated tumor cells at 3 h. Over time, the fluorescence intensity of each group continued to increase, with the variation becoming more significant. The maximum fluorescence enhancement in acid-treated tumor cells was more than 2-fold compared to untreated tumor cells. This comparative analysis of fluorescence intensity confirmed that the imine and disulfide bonds in the beta-CD nanocage played a key role in drug release. Furthermore, the acidic and reductive tumor microenvironment acted as a driver for a controlled drug release pathway.

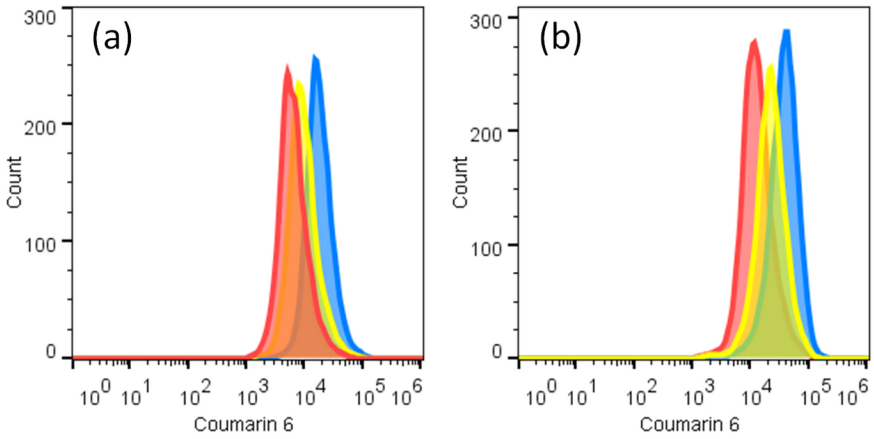

Figure 9 The flow cytometry analysis for treating SKOV3 cells with coumarin 6 loaded beta-CD nanocage in acidic environment, reduction environment and normal physiological environment for 3 h (a) and 6 h (b) respectively.

4. Conclusion

The proposed biodegradable covalent beta-CD nanocage-like structure was constructed using aldehyde group functionalized beta-CD and cystamine in a straightforward manner. Characterization of the prepared beta-CD nanocage was conducted using ^{1}H NMR, FTIR, AFM, and DLS. Overall, our results demonstrate that DOX-loaded beta-CD nanocage exhibited acid-responsive and reductive-responsive drug release, attributed to the presence of imine and disulfide linkages. Furthermore, in cultured tumor cells with specific upregulation of acid and GSH, DOX-loaded beta-CD nanocage showed enhanced tumor cell killing, as confirmed by cell viability assays. Cellular fluorescence imaging and flow cytometry analyses supported these findings, indicating that beta-CD nanocage enables drug release under acidic and reductive conditions, enhancing chemotherapy effectiveness. In conclusion, our study suggests that beta-CD-based drug delivery systems hold promise for addressing medical challenges and advancing nanomedicine applications in tumor treatment.

Conflicts of Interest

The authors declare no conflicts of interest.

Data availability

Data will be made available on request.

Acknowledgement

This work was supported by the Scientific Research Fund of Hunan Provincial Education Department (No. 202401000891), National College Students' Innovation and Entrepreneurship Training Program, China (No. S202310534001 and S202310534137), Key Science and Technology Project of Nanjing Municipal Administration for Market Regulation (No. Kj2022048), Science and Technology Plan Project of Jiangsu Provincial Administration for Market Regulation (No. KJ2023036 and KJ21125048).

References

[1] J. Wankar, N.G. Kotla, S. Gera, S. Rasala, A. Pandit, Y.A. Rochev, Recent Advances in Host–Guest Self-Assembled Cyclodextrin Carriers: Implications for Responsive Drug Delivery and Biomedical Engineering, Adv. Funct. Mater. 30(44) (2020).[2] H. Zhang, T. Zhang, X. Huang, C. Liu, S. Ma, S. Li, Y. Li, J. Liu, Z. Du, M. Yang, Oral Synergism of Egg-White-Derived Peptides (EWDP) and Curcumin for Colitis Mitigation via Polysaccharide/Cyclodextrin Metal–Organic Framework-Based Assemblies, J. Agric. Food Chem.

72(19) (2024) 11140-11152.[3] J.-B. Hou, X.-Q. Zhang, D. Wu, J.-F. Feng, D. Ke, B.-J. Li, S. Zhang, Tough Self-Healing Elastomers Based on the Host–Guest Interaction of Polycyclodextrin, ACS Appl. Mater. Interfaces 11(12) (2019) 12105-12113.[4] A. Shukla, A.P. Singh, B. Ray, V. Aswal, A.G. Kar, P. Maiti, Efficacy of polyurethane graft on cyclodextrin to control drug release for tumor treatment, J. Colloid Interface Sci. 534 (2019) 215-227.[5] C. Ouyang, M. Deng, X. Tan, Z. Liu, T. Huang, S. Yu, Z. Ge, Y. Zhang, Y. Ding, H. Chen, H. Chu, J. Chen, Tailored design of NHS–SS–NHS cross-linked chitosan nano-hydrogels for enhanced anti-tumor efficacy by GSH-responsive drug release, Biomed. Mater. 19(4) (2024) 045015.[6] S. Zhang, S. Zhou, H. Liu, M. Xing, B. Ding, B. Li, Pinecone-Inspired Nanoarchitectured Smart Microcages Enable Nano/Microparticle Drug Delivery, Adv. Funct. Mater. 30(28) (2020) 2002434.[7] Y. Zhang, T. Huang, W. Lv, K. Yang, C. Ouyang, M. Deng, R. Yi, H. Chu, J. Chen, Controlled growth of titanium dioxide nanotubes for doxorubicin loading and studies of in vitro antitumor activity, Frontiers in Bioengineering and Biotechnology 11 (2023).[8] W. Lv, K. Yang, J. Yu, Y. Wu, M. Zhang, Z. Liu, X. Wang, J. Zhou, H. Ma, R. Yi, H. Chu, J. Chen, A generalizable strategy for crosslinkable albumin-based hydrogels and application as potential anti-tumor nanoplatform, J. Biomater. Appl. 37(10) (2023) 1813-1822.[9] M. Deng, C. Ouyang, K. Yang, W. Lv, T. Huang, X. Li, M. Zhou, H. Wu, M. Xie, P. Shi, K. Gao, R. Yi, W. Peng, H. Chu, J. Chen, An acid-labile bridged -CD-based nano-hydrogel with superior anti-tumor drug delivery and release capacity, J. Drug Delivery Sci. Technol. 78 (2022) 103953.[10] J. Chen, H. Liu, X. Li, J. Li, R. Tang, Z. Deng, Y. Yang, S. Zhong, Dually acid- and GSH-triggered bis(-cyclodextrin) as drugs delivery nanoplatform for effective anticancer monotherapy, Nanotechnology 32(14) (2021) 145714.[11] R. Xiao, G. Zhou, Y. Wen, J. Ye, X. Li, X. Wang, Recent advances on stimuli-responsive biopolymer-based nanocomposites for drug delivery, Composites, Part B 266 (2023) 111018.[12] Z. Liu, L. Ye, J. Xi, J. Wang, Z. Feng, Cyclodextrin polymers: Structure, synthesis, and use as drug carriers, Prog. Polym. Sci. 118 (2021) 101408.[13] S.S. Braga, Cyclodextrin superstructures for drug delivery, J. Drug Delivery Sci. Technol. 75 (2022) 103650.[14] Q. Liang, J. Ye, Y. Wang, J. Wen, Y. Zhang, Z. Xu, Y. Chen, Y. Zhang, Z. Chen, S. Li, L. Weng, D. Zhang, X. Zhao, An enzyme-free and ratiometric biosensor for single nucleotide polymorphism with portable electrochemical system, Sensors and Actuators B: Chemical 412 (2024) 135745.[15] Y. Zhang, S. Xu, M. Luo, J. Chen, L. Wang, F. Yang, J. Ye, J. Liu, B. He, L. Weng, S. Li, D. Zhang, Hairpin-Empowered Invasive Reaction Combined with Catalytic Hairpin Assembly Cascade Amplification for the Specific Detection of Single-Nucleotide Polymorphisms, Analytical Chemistry (2024).[16] W. Cheng, M. Luo, Y. Zhang, J. Ye, J. Wan, Y. Zou, X. Zhao, Z. Chen, S. Li, D. Zhang, In situ quantitative mapping of coding single nucleotide polymorphism on mRNA inside cells by SERS-fluorescence dual-mode probe, Sensors and Actuators B: Chemical 413 (2024) 135871.[17] J. Ye, M. Fan, J. Zhan, X. Zhang, S. Lu, M. Chai, Y. Zhang, X. Zhao, S. Li, D. Zhang, In silico bioactivity prediction of proteins interacting with graphene-based nanomaterials guides rational design of biosensor, Talanta 277 (2024) 126397.[18] Y. Zhang, Q. Jiang, M. Wojnilowicz, S. Pan, Y. Ju, W. Zhang, J. Liu, R. Zhuo, X. Jiang, Acid-sensitive poly(-cyclodextrin)-based multifunctional supramolecular gene vector, Polym. Chem. 9(4) (2018) 450-462.[19] C. Chen, Y. Chen, X. Dai, J. Li, S. Jia, S. Wang, Y. Liu, Multicharge -cyclodextrin supramolecular assembly for ATP capture and drug release, Chem. Commun. 57 (2021) 2812-2815.[20] D. Colesnic, P.J. Hernando, L.M. Chamoreau, L. Bouteiller, M. Ménand, M. Sollogoub, Precisely Designed Difunctionalized Cyclodextrin Produces a Solid-State Organic Porous Hierarchical Supramolecular Assembly, Chem. - Eur. J. 29(35) (2023) e202300150.[21] Y. Zhang, L. Wang, J. Ye, J. Chen, S. Xu, S. Bu, M. Deng, L. Bian, X. Zhao, C. Zhang, L. Weng, D. Zhang, Rationally Designed Dual Base Pair Mismatch Enables Toehold-Mediated Strand Displacement to Efficiently Recognize Single-Nucleotide Polymorphism without Enzymes, Anal. Chem. 96(1) (2023) 554-563.[22] Y. Zhang, S. Xu, J. Chen, L. Wang, L. Bian, J. ye, L. Weng, X. Zhao, C.-T. Lin, S. Li, D. Zhang, A biosensor using semi-DNA walker and CHA -FRET

loop for ultrasensitive detection of single nucleotide polymorphism, Sens. Actuators, B 400 (2024) 134908.[23] C. Lou, X. Tian, H. Deng, Y. Wang, X. Jiang, Dialdehyde--cyclodextrin-crosslinked carboxymethyl chitosan hydrogel for drug release, Carbohydr. Polym. 231 (2020) 115678.[24] A. Bergal, M. Andac, Detailed investigation and influence of oxidation degree on synthesis, characterization and antibacterial activity of - cyclodextrin, Carbohydr. Res. 533 (2023) 108936.[25] J. Wang, Z. Guo, J. Xiong, D. Wu, S. Li, Y. Tao, Y. Qin, Y. Kong, Facile synthesis of chitosan-grafted beta-cyclodextrin for stimuli-responsive drug delivery, Int. J. Biol. Macromol. 125 (2019) 941-947.[26] Y. Yu, Q. Wang, J. Yuan, X. Fan, P. Wang, A novel approach for grafting of -cyclodextrin onto wool via laccase/TEMPO oxidation, Carbohydr. Polym. 153 (2016) 463-470.[27] A.A. Makki, F. Bonnier, R. Respaud, F. Chtara, A. Tfayli, C. Tauber, D. Bertrand, H.J. Byrne, E. Mohammed, I. Chourpa, Qualitative and quantitative analysis of therapeutic solutions using Raman and infrared spectroscopy, Spectrochim. Acta, Part A 218 (2019) 97-108.[28] T. Wang, L. Wang, X. Li, X. Hu, Y. Han, Y. Luo, Z. Wang, Q. Li, A. Aldalbahi, L. Wang, S. Song, C. Fan, Y. Zhao, M. Wang, N. Chen, Size-Dependent Regulation of Intracellular Trafficking of Polystyrene Nanoparticle-Based Drug-Delivery Systems, ACS Appl. Mater. Interfaces 9(22) (2017) 18619-18625.[29] S. Acter, M.L.P. Vidallon, S. Crawford, R.F. Tabor, B.M. Teo, Bowl-Shaped Mesoporous Polydopamine Nanoparticles for Size-Dependent Endocytosis into HeLa Cells, ACS Appl. Nano Mater. 4(9) (2021) 9536-9546.